

# Carrier Proteins Determine Local Pharmacokinetics and Arterial Distribution of Paclitaxel

MARK A. LOVICH,<sup>1,2</sup> CHRIS CREEL,<sup>1</sup> KRISTY HONG,<sup>1</sup> CHAO-WEI HWANG,<sup>1</sup> ELAZER R. EDELMAN<sup>1,3</sup>

<sup>1</sup>Harvard-MIT Division of Health Sciences and Technology, Massachusetts Institute of Technology, Room 16-343, Cambridge, Massachusetts 02139

<sup>2</sup>Department of Anesthesia and Critical Care, Massachusetts General Hospital, Boston, Massachusetts 02114

<sup>3</sup>Cardiovascular Division, Department of Medicine, Brigham and Women's Hospital, Harvard Medical School, Boston, Massachusetts 02115

Received 7 September 2000; revised 21 December 2000; accepted 6 April 2001

**ABSTRACT:** The growing use of local drug delivery to vascular tissues has increased interest in hydrophobic compounds. The binding of these drugs to serum proteins raises their levels in solution, but hinders their distribution through tissues. Inside the arterial interstitium, viscous and steric forces and binding interactions impede drug motion. As such, this might be the ideal scenario for increasing the amount of drug delivered to, and residence time within, arterial tissues. We quantified carrier-mediated transport for paclitaxel, a model hydrophobic agent with potential use in proliferative vascular diseases, by determining, in the presence or absence of carrier proteins, the maximum concentration of drug in aqueous solution, the diffusivity in free solution, and the diffusivity in arterial tissues. Whereas solubility of paclitaxel was raised 8.1-, 21-, and 57-fold by physiologic levels of  $\alpha_1$ -acid glycoproteins, bovine serum albumin, and calf serum over that in protein-free solution, diffusivity of paclitaxel in free solution was reduced by 41, 49, and 74%, respectively. When paclitaxel mixed in these solutions was applied to arteries both *in vitro* and *in vivo*, drug was more abundant at the tissue interface, but protein carriers tended to retain drug in the lumen. Once within the tissue, these proteins did not affect the rate at which drug traverses the tissue because this hydrophobic drug interacted with the abundant fixed proteins and binding sites. The protein binding properties of hydrophobic compounds allow for beneficial effects on transvascular transport, deposition, and distribution, and may enable prolonged effect and rationally guide local and systemic strategies for their administration. © 2001 Wiley-Liss, Inc. and the American Pharmaceutical Association *J Pharm Sci* 90:1324–1335, 2001

**Keywords:** paclitaxel; solubility; diffusion; carrier protein-mediated transport; vascular pharmacokinetics

## INTRODUCTION

There is burgeoning interest in the potential of combined mechano-pharmacologic therapy to improve the clinical outcome of mechanical revascu-

larization.<sup>1,2</sup> Indeed, a wide variety of compounds inhibit the proliferative neointimal response in animal models of arterial injury when applied locally from endovascular stents or implantable drug depots. Agents such as heparin,<sup>3–5</sup> dexamethasone,<sup>6,7</sup> angiotensin-converting enzyme inhibitors,<sup>8</sup> forskolin,<sup>9</sup> colchicine,<sup>10,11</sup> antisense oligonucleotides,<sup>12,13</sup> paclitaxel, and other anti-neoplastic drugs<sup>14–17</sup> span the full range of molecular weight, conformation, and molecular charge. These physicochemical properties deter-

Correspondence to: E. R. Edelman (Telephone: 617-253-1569; Fax: 617-253-2514; E-mail: eedelman@mit.edu)

*Journal of Pharmaceutical Sciences*, Vol. 90, 1324–1335 (2001)  
© 2001 Wiley-Liss, Inc. and the American Pharmaceutical Association

mine their circulation through the vasculature and penetration into blood vessels from local devices, and ultimately govern the applicability and utility of these compounds in treating proliferative vascular diseases. For example, small compounds diffuse through tissues faster than larger ones,<sup>18–21</sup> and charged molecules are highly soluble and thus rapidly diffuse into and out of tissues more readily than neutral hydrophobic compounds.<sup>22,23</sup>

In prior studies we defined local vascular pharmacokinetics by quantifying diffusive and convective mechanisms of transport, and nonspecific binding interactions by which hydrophilic compounds, such as heparin, distribute in and around blood vessels.<sup>22–27</sup> We found that although tissues could be easily loaded with soluble compounds they are cleared quite quickly by similar means.<sup>22</sup> In fact, unless administered continuously, these hydrophilic compounds are generally cleared well before they can exert their full pharmacologic effects.<sup>22,28</sup> Accordingly it was not surprising that there has been only limited clinical benefit from the local release of these compounds. Highly insoluble compounds, on the other hand, are administered to, distributed through, and cleared from tissues by fundamentally different mechanisms than soluble drugs, and for this reason are receiving markedly increased attention. For example, insoluble compounds are carried on serum albumin or  $\alpha_1$ -acid glycoprotein ( $\alpha$ GP) and association with these serum proteins may allow for them to be retained within the blood vessel, limiting their distribution from the vasculature to tissues.<sup>29–33</sup> We quantified the impact of protein-mediated transport on vascular tissue distribution with a highly insoluble model compound, paclitaxel,<sup>14,15</sup> an antiproliferative agent.

We characterized arterial uptake of carrier bound drugs as the net result of several discrete steps (Fig. 1). First we determined the effective solubility (Fig. 1, I) or the ability of the soluble protein carriers, such as albumin or  $\alpha$ GP, to increase the amount of drug in solution above that possible in the absence of such carriers. We then quantified how association with these carriers slows the diffusion of the drug in free aqueous solution (Fig. 1, II). We further demonstrated, in an *ex vivo* preparation, the complex interaction of drug, carrier, and tissues by assessing the drug distribution in arterial tissue (Fig. 1, III) and confirmed our findings *in vivo*. These analyses demonstrate rigorously how hydrophobic drugs

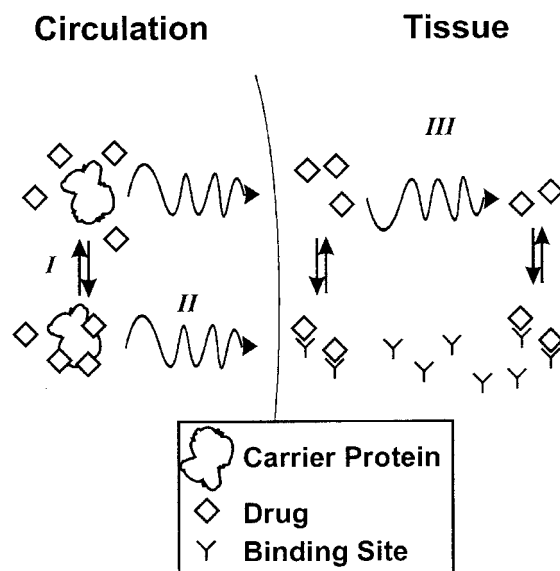


**Figure 1.** Schematic depiction of the impact of carrier proteins on hydrophobic drug in the circulation and in tissues. (I) The presence of carrier proteins allows more drug to be held in solution. (II) These proteins influence the motion of solutes by slowing their diffusion in free solution. (III) Once in the tissue interstitium there is competition between drug diffusion and reversible association to fixed hydrophobic binding sites, thus slowing the overall motion of the drug solute.

need the solubility of carriers for systemic circulation, and yet initial uptake and motion through tissues may be limited by the molecular properties of the carrier, highlighting the complexity of the local vascular pharmacokinetics of protein-bound drug. This approach and these data will be critical to realize the full potential of hydrophobic compound as they enter clinical trials for endovascular stent-based drug delivery.

## METHODS

### Effective Solubility

Nonspecific binding to soluble serum proteins may increase the maximum amount of paclitaxel that can be held in aqueous solutions. We tested this hypothesis by measuring the effective solubility of paclitaxel in phosphate buffered saline (PBS, Sigma), calf serum, (Life Technologies), bovine serum albumin (BSA, 4 g/dL, Fisher Scientific) in PBS, and bovine  $\alpha_1$ -acid glycoproteins ( $\alpha$ GP, 100mg%, Sigma) in PBS. Unlabeled

paclitaxel stock solutions were made from crystallized drug dissolved in ethanol (1.0 mg/mL). [<sup>3</sup>H]Paclitaxel (Amersham) was diluted in 100% ethanol to a working stock (0.1 μCi/mL, 0.047 μg/mL). Samples of these stock solutions were transferred into 1.5-mL centrifuge tubes so that the amount of [<sup>3</sup>H]paclitaxel was fixed (0.05–0.1 μCi) and the amount of unlabeled drug ranged from 1 to 1300 μg. Because trace quantities of solvents can dramatically affect paclitaxel solubility,<sup>34</sup> care was taken to remove all of the ethanol. The tubes were heated to 37°C under a nitrogen gas stream for 1 h, which was four times longer than it took for the ethanol to fully evaporate. One of the four solutions to be tested (PBS, 4% BSA, 0.1% αGP or serum; 1 mL) was added, the tubes were sealed and maintained at 37°C under gentle agitation for exactly 24 h. The incubation times were precisely standardized as the solubility of paclitaxel decreases over the first 24 h in solution with its transition from an anhydrous to dihydrate form.<sup>35,36</sup> The tubes were centrifuged at 5000 rpm for 5 min, and two 200-μL samples of supernatant were transferred to separate scintillation vials for measurement of the concentration of paclitaxel held in solution. Five milliliters of Hionic Fluor scintillation cocktail (Packard) was added to each vial, and the amount of [<sup>3</sup>H]paclitaxel determined via liquid scintillation spectroscopy (2500 TR Liquid Scintillation Analyzer, Packard-Canberra). Both of the concentration measurements from each centrifuge tube were averaged and considered a single measurement. Experiments were performed in triplicate. For each tested solution, unlabeled paclitaxel mass was increased in sequential experiments until the dissolved concentration was not statistically significantly different from the previous value using a Student's *t* test, and this plateau concentration was considered to be the effective solubility.

### Diffusivity in Free Solution

Association with soluble protein carriers increases the amount of hydrophobic drug in solution; however, these complexes may be larger, and therefore diffuse more slowly in free solution than drug alone because of increased viscous dissipation of kinetic energy. We used Franz diffusion cells (PermeGear) to measure the effective free diffusivity of [<sup>3</sup>H]paclitaxel in protein-free buffer (PBS), or in the presence of 100 mg% αGP in PBS, 4% BSA in PBS, or calf serum. A hydrophilic filter (GVWP, 0.22-μm pore diameter, 70% porosity,

125 μm thickness, Millipore) provided unstirred channels for drug diffusion from an upper source chamber (1 mL) to a bottom sink chamber (5 mL). The bottom chamber was well mixed with a magnetic stir bar. The diameter of the pores in the filter were 2 orders of magnitude wider than the molecular radius of the drug or proteins, and therefore the observed transport reflects the diffusion of paclitaxel in complexes with carriers in free solution.<sup>23</sup>

Aliquots of [<sup>3</sup>H]paclitaxel from stock solutions (200 μL, 1.0 μCi/mL, 0.47 μCi/mL) were placed in vials and the ethanol solvent was evaporated under a nitrogen stream at 37°C for 1 h. The test solution (4 mL) was added and stirred for 3 h at room temperature. One milliliter was transferred into the source chambers of three different diffusion cells at room temperature. For experiments with BSA, αGP, and serum, unlabeled paclitaxel was added (60, 20, and 150 μg/mL, respectively) so that the drug in the top source chamber was always near its effective solubility limit and the majority of drug in solution was therefore protein bound. The solution in the bottom-sink chamber was identical to that in the top except that [<sup>3</sup>H]paclitaxel was omitted. Samples (10 μL) were removed from both top and bottom chambers at regular intervals for up to 4 h and the concentration of [<sup>3</sup>H]paclitaxel in each sample was determined via liquid scintillation spectroscopy. In between sample collection, the openings to each chamber were covered with Parafilm (American National Can) to prevent evaporation. For comparison, the transport of [<sup>14</sup>C]BSA (NEN Life) across the filter in these diffusion cells was measured by similar techniques as used for paclitaxel.

The time rate of change of [<sup>3</sup>H]paclitaxel or [<sup>14</sup>C]BSA concentration in the bottom sink chamber ( $dc_b/dt$ ) was calculated from a linear regression over the steady-state portion of the concentration measurements. From a mass balance for the bottom chamber and Fick's law of diffusion within the pores of the filter, the diffusivity of paclitaxel in solution ( $D_o$ ) in association with available protein carriers is as follows:<sup>23</sup>

$$D_o = \frac{lV_b}{c_t A_o} \frac{dc_b}{dt} \quad (1)$$

where  $V_b$  is the volume of the lower chamber,  $A_o$  is the total open area of the filter computed as the filter area multiplied by the porosity,  $l$  is the thickness of the filter, and  $c_t$  is the average

[<sup>3</sup>H]paclitaxel concentration in the upper chamber, which never decreased > 10% over the course of the experiment. All experiments were performed in triplicate, and the measured diffusivities under each set of conditions were averaged. ANOVA was used to determine if measured diffusivities were statistically distinguishable.

### Distribution in Arterial Tissues

We examined the transmural [<sup>3</sup>H]paclitaxel distribution in freshly explanted calf carotid arteries with endovascular application of drug in protein-free Krebs-Henseleit Buffer (KH, Sigma), 4% BSA in KH buffer, or in calf serum in an *ex vivo* perfusion apparatus that simulated plasma flow through the lumen.<sup>23,26,37</sup> Calf common carotid arteries were harvested at a slaughterhouse and transported in PBS (Sigma) at 4°C. The arteries were cleaned of excess fat and fascia, and gently cannulated with polyethylene tubing (2.08-mm o.d., Becton Dickinson). The integrity of the artery was assessed by connecting one cannula to an elevated bag of PBS, sealing the other cannula, and inspecting for leaks under a dissecting microscope.<sup>23,26,37</sup>

### Perfusion Apparatus

An *ex vivo* perfusion apparatus was constructed wherein the arterial wall separated endovascular and perivascular fluid compartments in which the concentration of drugs could be precisely controlled and monitored. The perfusion apparatus allowed perfusate from an upper reservoir to flow through three separate Tygon tubes (MasterFlex Tygon Tubing, Lab Grade, 3.1 mm i.d., Cole-Palmer) into three arteries, and then through three throttle valves before emptying into one common lower reservoir.<sup>23,26,37</sup> The perfusate was then pumped (MasterFlex L/S Economy Pump, Cole-Palmer) to the upper reservoir, completing an endovascular circuit. The transmural pressure gradient was set by the relative height, hydrostatic head ( $\Delta H$ ), of the upper reservoir and the downstream resistance imparted by the throttle valves. An overflow line connected the upper and lower reservoirs and held the hydrostatic head constant regardless of pump speed. The three arteries were immersed in a single perivascular bath of KH buffer that was stirred and maintained at 37°C with a heat exchanger. The entire perfusion apparatus was placed in a closed chamber that was maintained at 37°C and 100% re-

lative humidity. The volumetric flow rate through the lumen of each artery was maintained at ~0.65 mL/s during all experiments. Each of the three endovascular circuits had a volume of 75 mL, and the perivascular bath volume was 1000 mL.

### Perfusion

The ethanol solvent was removed from [<sup>3</sup>H]paclitaxel with a nitrogen gas stream for 1 h in a 100 mL glass vial. Perfusate was added, and the paclitaxel was dissolved for 2 h under agitation (0.1  $\mu$ Ci/mL, 0.047  $\mu$ g/mL). The perfusate was transferred to the lower reservoir of the perfusion apparatus. The flow through the endovascular circuit was initiated with the arterial cannula connectors bypassed, and the system was allowed to warm up and equilibrate for 2 h. The height of the upper reservoir was set even with the arteries ( $\Delta H = 0$ ) and therefore no transmural pressure gradient was applied. Three arteries were perfused in parallel for 4 h. At regular intervals, 100  $\mu$ L was removed from both the perivascular and endovascular compartments for determination of the [<sup>3</sup>H]paclitaxel concentration by liquid scintillation spectroscopy using Hionic-Fluor (Packard). Perivascular contamination with radioactivity was considered a breach in arterial integrity, and all associated samples were discarded and the experiment repeated.

### Harvesting

After each experiment, the arteries were quickly removed from the perfusion system and the cannulated ends were removed with a razor blade. The artery was cut longitudinally and laid flat between two glass slides separated by 1.5-mm spacers. OCT Embedding Medium (Tissue-Tek, Sakura Finetechnical) was applied around the edges of the tissue and on the adventitial surface prior to placement of the top slide. Evans Blue Dye (Sigma) was mixed with the OCT to help determine the location of the tissue border during subsequent sectioning. The slides were clamped together and the artery was snap-frozen with cryospray (Cytocool II, VWR Scientific) and stored in a -80°C freezer until sectioning. No more than 90 s elapsed between the termination of perfusion and freezing of all three arteries.

### Transmural Cryosectioning

The arterial distribution of paclitaxel was determined by sectioning the tissues parallel to the

intima with a refrigerated microtome (Cryotome SME, Shandon Inc.) using previously described techniques.<sup>37,38</sup> Each sample was removed from the glass slide encasements, immediately placed on a cryobar at  $-59^{\circ}\text{C}$ , and trimmed to a rectangular shape. The sample was transferred to another glass slide with the intima oriented up and warmed with gentle exhalation until liquid was observed on the tissue surface. The liquid was gently blotted (Kimwipes EX-L, Kimberly-Clark) to remove adsorbed perfusate. The rectangular sample was immediately placed on a pre-leveled cryotome chuck made from OCT at  $-25^{\circ}\text{C}$ , and the length and width were measured with a caliper. OCT Embedding Medium was applied around the edges of the sample and chuck to add support while cutting. Twenty-micrometer thick sections were cut parallel to the intima and placed in individual glass scintillation vials that were pre-cooled to  $-25^{\circ}\text{C}$ . Sections were digested with 750  $\mu\text{L}$  of Soluene-350 (Packard-Canberra) at room temperature for 72 h. Liquid scintillation cocktail (5 mL, Hionic-Fluor) was added to each sample vial and the [ $^3\text{H}$ ]paclitaxel content determined by liquid scintillation spectroscopy. The tissue concentration at each transmural location was calculated as the mass of paclitaxel normalized by the measured tissue area and slice thickness.

### Arterial Uptake *In Vivo*

To verify that our findings were not specific to our *ex vivo* preparation and represented real physiological phenomena, we delivered paclitaxel to rat carotid arteries *in vivo* in either calf serum or in protein-free KH buffer. Male Sprague Dawley rats (325–400 g, Charles River) were anesthetized with an intraperitoneal injection of ketamine (75 mg/kg) and xylazine (5 mg/kg). A midline neck incision exposed the left common and external carotid arteries. A catheter made from polyethylene tubing (0.965 mm o.d., Becton Dickinson) was introduced into the external carotid artery through an arteriotomy and secured with a ligature. The delivery solution with [ $^3\text{H}$ ]paclitaxel (0.1  $\mu\text{Ci/mL}$ , 0.047  $\mu\text{g/mL}$ ) was suspended from an elevated bag (120 cm) and the intra-arterial line was purged of air. The internal carotid artery was ligated, and the solution was flushed into the common carotid artery. A proximal ligature on the common carotid artery was tightened to prevent blood from reentering the vessel and to maintain the pressure. The arterial wall was exposed to

paclitaxel in the lumen for 15 min. Pilot experiments demonstrated that this time was sufficient for paclitaxel to traverse the rat carotid artery and for steady state to be established. Following the infusion, the internal, external, and proximal-common carotid arteries were cut with dissecting scissors between the double ligatures in such a way that blood did not contaminate the artery and the test solution did not leak out. The fluid from the lumen of the artery was aspirated through the cannula, and a sample was weighed and assayed for [ $^3\text{H}$ ]paclitaxel content. The endovascular concentration ( $c_{ev}$ ) was calculated as the mass of drug per unit volume of aspirated fluid, assuming a density of 1 mg/mL. The lumen of the common carotid artery was flushed with 3 mL of PBS. The thinness of the rat carotid artery ( $\sim 40\ \mu\text{m}$ ) precluded use of the transmural sectioning technique and in its place we measured the deposition in the whole arterial segment. The artery was weighed wet, digested with Soluene-350 at  $60^{\circ}\text{C}$  for 6 h, and assayed for [ $^3\text{H}$ ]paclitaxel content.

For direct comparison, paclitaxel was administered in either calf serum or in protein-free KH buffer to calf carotid arteries *ex vivo* with a pressure gradient of 90 mmHg, for 15 min. Endovascular samples of perfusate were taken at the beginning and end of the experiment, and the measured paclitaxel concentration was averaged. Following removal from the perfusion system the arteries were flushed with PBS, weighed wet, digested with Soluene-350 without transmural sectioning, and assayed for [ $^3\text{H}$ ]paclitaxel concentrations in the whole arterial segment. The whole artery deposition of paclitaxel in rat carotid arteries *in vivo* or calf carotid arteries *ex vivo* were expressed as mean  $\pm$  standard deviation (SD). The Student's *t* test was used to determine if the difference in deposition between application in protein free buffer or serum was significant.

## RESULTS

### Effective Solubility

The effective solubility, the maximum amount of drug held in solution, was considered to be the plateau in soluble concentration as more drug was added to a closed system (Table 1). In the absence of added proteins, paclitaxel reached a maximal concentration of  $3.0 \pm 0.7\ \mu\text{g/mL}$  in PBS.

**Table 1.** Effective Solubility, Free Diffusivity, and Effective Diffusivity in Arterial Media of Paclitaxel in the Presence of Protein Carriers<sup>a</sup>

Test Solutions of Paclitaxel in:	Effective Solubility ( $\mu\text{g/mL}$ )	Free Diffusivity ( $D_o$ , $\mu\text{m}^2/\text{s}$ )	Effective Diffusivity in Arterial Media ( $D_{\text{art}}$ , $\mu\text{m}^2/\text{s}$ )
Protein-free buffer	$3.0 \pm 0.7$	$76.6 \pm 6.1$	$0.22 \pm 0.08$
4% Albumin	$64.5 \pm 0.2$	$38.9 \pm 3.9$	$0.23 \pm 0.05$
0.1% $\alpha_1$ -Acid glycoproteins	$24.3 \pm 4.0$	$45.4 \pm 7.2$	
Calf serum	$171 \pm 9.3$	$20.3 \pm 4.0$	$0.21 \pm 0.02$

<sup>a</sup>Results are expressed as mean  $\pm$  standard deviation.

This value represented  $\sim 2\%$  of the drug in the centrifuge tube, the remainder presumably being precipitated or adsorbed to the tube. In 4% BSA the concentration of paclitaxel in solution was  $64.5 \pm 0.2 \mu\text{g/mL}$ , a 21.3-fold increase over the solubility without protein carriers.  $\alpha\text{GP}$  in physiologic concentration (100 mg/dL) raised the effective solubility to  $24.3 \pm 4.0 \mu\text{g/mL}$ , an increase of 8.1-fold over the solubility without proteins. In serum, the effective solubility rose 57-fold over protein-free buffer to  $171 \pm 9 \mu\text{g/mL}$ , indicating that paclitaxel binds many other less abundant serum proteins than those studied.

### Diffusivity in Solution

The diffusivity of paclitaxel in free solution ( $D_o$ ) in the presence and absence of protein carriers was assessed in a Franz diffusion cell. The paclitaxel concentration in the sink chamber normalized by the average concentration in the source is shown over time (Fig. 2). Because the chamber volumes and filter dimensions were fixed in all of these experiments, the slope as determined by a least-squares method is proportional to the diffusivity of paclitaxel in free solution (eq. 1). In the absence of serum proteins, the diffusivity of paclitaxel is  $76.6 \pm 6.1 \mu\text{m}^2/\text{s}$  (Table 1). In the presence of  $\alpha\text{GP}$  (100 mg/dL) the diffusivity was  $45.4 \pm 7.2 \mu\text{m}^2/\text{s}$ , 40.7% lower than in protein-free buffer. When dissolved in a 4% albumin solution, paclitaxel diffused at a rate of  $38.9 \pm 6.7 \mu\text{m}^2/\text{s}$ , 49.2% lower than in protein free solution. In serum the diffusivity was  $20.3 \pm 7.0 \mu\text{m}^2/\text{s}$ , 73.5% lower than in protein-free buffer. Thus, the larger the proteins that paclitaxel is exposed to, the lower the diffusivity in free aqueous solutions. ANOVA showed that all of these measured diffusivities in free solution were unique ( $p < 0.01$ ). The diffusivity of [<sup>14</sup>C]BSA in free solution was  $57.5 \pm 8.3 \mu\text{m}^2/\text{s}$ , which is somewhat faster than [<sup>3</sup>H]paclitaxel in the presence of 4% albumin, and

close to that of albumin alone as measured by others.<sup>39</sup>

### Distribution in the Arterial Wall

The distribution of paclitaxel in the calf carotid artery 4 h after administration *ex vivo* is shown normalized by the endovascular driving concentration (Fig. 3). For all test solutions, the concentration of paclitaxel near the intima was much larger than the endovascular driving concentration ( $c_T(0)/c_{\text{ev}} \gg 1$ ), and decreases with distance from the lumen. The normalized intimal tissue concentration was highest for application without proteins (KH), where tissue concentrations were close to 100-fold above perfusate concentration. Arterial concentrations of paclitaxel applied in serum were lowest relative to the endovascular concentrations.

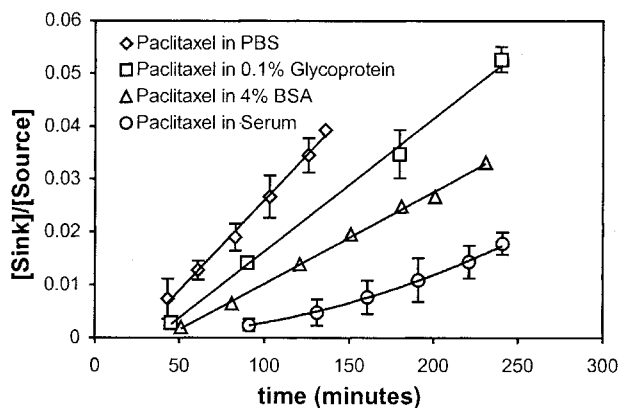


**Figure 2.** [<sup>3</sup>H]Paclitaxel concentration in the lower sink chamber normalized by the top source concentration of a Franz diffusion cell in PBS, 0.1%  $\alpha\text{GP}$  in PBS, 4% BSA in PBS, and calf serum ( $n = 3$ ,  $\pm\text{SD}$ ). Lines in the figure are fit to the data using a least-squares method. The slope is proportional to the free diffusivity ( $D_o$ , Table 1) in the presence of carriers. Unlabeled paclitaxel was added to both chambers so that the drug was near its solubility limit (see text).

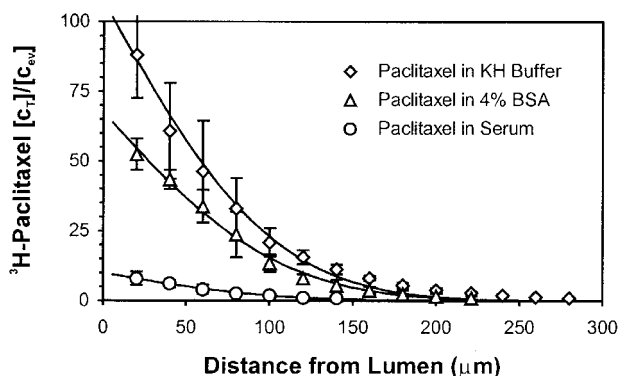


**Figure 3.** Tissue concentration of paclitaxel normalized by the corresponding endovascular concentration ( $c_T/c_{ev}$ ) as a function of distance from the intima in *ex vivo* calf carotid arteries. Paclitaxel was applied to the endovascular surface for 4 h in either protein-free Krebs Henseleit buffer (KH), 4% BSA, or calf serum at 37°C with no transmural pressure gradient ( $n = 3$ ,  $\pm$ SD). The lines are fits to the Complementary Gauss Error Function (erfc) using a Nelder–Meade Algorithm.

### In Vivo

Paclitaxel was delivered in either protein-free KH buffer or in calf serum to the endovascular surface of the rat carotid artery *in vivo* for 15 min. For comparison, paclitaxel was administered to calf carotid arteries *ex vivo* for 15 min. In both cases, the whole artery deposition was measured and normalized by the endovascular concentration (Fig. 4). Although the paclitaxel uptake was 3.5-fold greater *in vivo* than *ex vivo*, delivery to the arterial wall of the drug in protein-free KH buffer resulted in an 8.9- ( $p < 0.05$ ) and 8.6- ( $p < 0.05$ ) fold more efficient uptake than when delivered in calf serum, respectively. Although differences between the uptake *in vivo* and *ex vivo* may be attributed to different animal models, the consistent difference between the presence and absence of serum proteins suggests that the mechanisms of carrier-mediated transport are similar in both preparations.

## DISCUSSION

The local vascular pharmacokinetics for soluble hydrophilic and insoluble hydrophobic drugs depend on fundamentally different mechanisms. Whereas the former readily penetrates and diffuses across tissues, the latter interacts with soluble proteins within the systemic circulation

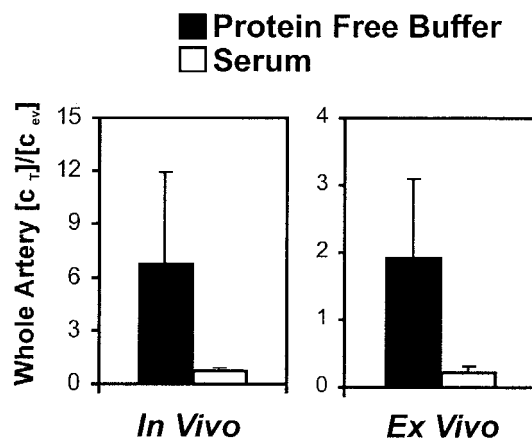


**Figure 4.** The whole artery deposition ( $c_T/c_{ev}$ ) of paclitaxel *in vivo* in the rat carotid artery and *ex vivo* in the calf carotid artery after administration in protein-free buffer and serum for 15 minutes, with a physiologic pressure gradient of 90 mmHg ( $n = 3$ ,  $\pm$ SD). Note the different scales used *in vivo* and *ex vivo*.

and with both fixed and soluble proteins in the tissue interstitium. We attempted to describe and quantify carrier-mediated protein transport in terms of several discrete mechanisms (Fig. 1). Protein carriers elevate levels of hydrophobic drug in the circulation (Fig. 1, I) and yet limit their free motion or diffusion (Fig. 1, II) and uptake by tissues. In the interstitium of tissues, there is a perpetual competition between reversible binding to fixed sites and forward diffusion within the interstitium (Fig. 1, III). We examined these mechanisms in arterial tissues using paclitaxel, an ideal model hydrophobic compound with profound potential in treating proliferative vascular diseases.

### Effective Solubility

The physical chemistry of paclitaxel is complex and has been studied in some detail.<sup>34–36,40</sup> Paclitaxel is hydrophobic and therefore highly insoluble in aqueous solutions, but very soluble in organic solvents. Reports of paclitaxel solubility in aqueous solutions range from 0.7 to 30  $\mu$ g/mL,<sup>41–43</sup> and has been shown to decrease 18-fold over a 24-h period.<sup>36</sup> Paclitaxel may exist in either an anhydrous form or as a stable dihydrate with an even lower solubility. The time dependence of the solubility may reflect conversion from the former to the latter.<sup>35,36</sup> Our effective solubility measurements were made after paclitaxel was

allowed to equilibrate with the test solution for 24 h.

Kumar et al.<sup>40</sup> showed that the unbound fraction of paclitaxel at 0.6  $\mu\text{M}$  was 5.3% in serum, 15.7% in human serum albumin, and 25.3% in  $\alpha\text{GPs}$ .<sup>40</sup> Whereas these values are most applicable to a single dose or concentration of drug, our data addresses the slightly different but important question of how much additional drug can be held in solution when more or additional species of proteins are present. Whereas  $\alpha\text{GP}$  raised the effective solubility of paclitaxel 8.1-fold over protein-free buffer, it only accounted for 14% of the increase seen with serum. Similarly, albumin raised paclitaxel levels 21-fold over protein-free buffer, but only accounted for 37% of the increase seen with serum (Table 1). These results suggest that although albumin is the major carrier of paclitaxel, it is by no means the only one.<sup>40</sup> Many other serum proteins may carry paclitaxel in small amounts, likely as a result of their lower serum concentrations. Our data demonstrates that although albumin is 40-fold more abundant in serum by mass than  $\alpha\text{GP}$ , it supports only three times as much paclitaxel. Therefore, albumin appears to be the dominant carrier of paclitaxel by virtue of the large number of available particles rather than a stronger binding avidity. Several have noted that the binding of hydrophobic drug is, in many cases, nonspecific and reversible.<sup>31,32,40</sup>

### Diffusivity in Solution

We used Franz diffusion cells to measure [<sup>3</sup>H]paclitaxel diffusivity in free solutions containing no protein, albumin,  $\alpha\text{GP}$ , or all the serum proteins. Our data show that there is an inverse relationship between the molecular weight of the carrier and the diffusivity of the paclitaxel–protein complex. The average molecular weights of paclitaxel,  $\alpha\text{GP}$ , albumin, and serum are 854 Da, 48 kDa, 67 kDa, and  $\sim 90$  kDa,<sup>39</sup> respectively, and the corresponding diffusivities of paclitaxel in protein-free buffer,  $\alpha\text{GP}$  solution, albumin solution, and serum are 76.6, 38.9, 45.4, and 20.3  $\mu\text{m}^2/\text{s}$  (Table 1). The free diffusivities of any globular solute is related to molecular size through the Stokes–Einstein relation, which balances viscous drag with the inertia from random thermal motion:<sup>44</sup>

$$D_o = \frac{RT}{6\pi\mu r_o} \quad (2)$$

where  $D_o$  is the free diffusivity,  $R$  is the Boltzmann constant,  $T$  is the absolute temperature,  $\mu$  is the solvent viscosity and  $r_o$  is the average molecular radius of the solute. Globular proteins with larger molecular weights have larger molecular radii and therefore diffuse slower because of greater viscous dissipation of kinetic energy. In this case, the solute is the drug–carrier complex and our measurements follow the transport of the [<sup>3</sup>H]paclitaxel, not the carriers. This demonstration quantifies how soluble carrier proteins allow more hydrophobic drug to be held in solution at the expense of slower diffusive motion through increased viscous drag.

The shape of the accumulation curve in the receiving chamber for paclitaxel serum is nonlinear, as the slope increases with time (Fig. 3). This result may indicate that the drug is associating with serum proteins of many different sizes and is traversing the filter according to the free diffusivity of each protein–drug complex. With time, successively larger proteins arrive in the receiving chamber, leading to increasing rates of paclitaxel transfer. The transport of paclitaxel in serum is slower than in albumin, suggesting that most of the binding is to serum proteins larger than albumin. The average molecular weight of the solutes in serum has been estimated to be  $\sim 90$  kDa.<sup>39</sup> Larger proteins may have more nonspecific binding sites for paclitaxel, and may thus dominate the observed drug transport.

### Distribution Into Tissues

Our tissue distribution data shows that paclitaxel undergoes significant binding to arterial tissues. The tissue concentration normalized by the driving endovascular concentration is almost always  $> 1$ , and reaches values close to 100. Drug enters the porous interstitium of tissues and soluble drug occupies the accessible or void volume at a concentration close to the applied, in this case endovascular, concentration. The only way for the tissue concentration to so greatly exceed the applied concentration is for there to be tremendous association with tissue elements along the void spaces within the interstitium. In addition to binding to fixed proteins within the arterial wall, paclitaxel associates with or partitions into hydrophobic structures such as lipid and cellular membrane. These associations impede the motion of paclitaxel down its concentration gradient, as there is a competition between forward diffusion



of soluble drug and reversible binding and dissociation (Fig. 1, III).

To quantify this impeded motion we calculated the "effective diffusivity" in arterial media ( $D_{\text{art}}$ ), which describes the net effects of diffusion in the void spaces of the interstitium and reversible binding to fixed elements. These values were estimated by using a Nelder–Meade Simplex algorithm provided by Matlab 5.3 (Mathworks, Natick, MA) to fit the transmural concentration profiles (Fig. 3) to the following:<sup>45</sup>

$$\frac{c_T(x)}{c_{\text{ev}}} = B_1 \operatorname{erfc}\left(\frac{x}{2\sqrt{D_{\text{art}}t}}\right) \quad (3)$$

which is the closed form solution for the problem of diffusion into a semi-infinite medium from a constant source at the boundary, where  $\operatorname{erfc}$  is the complementary Gauss error function.<sup>45</sup> Because paclitaxel did not completely traverse the arterial media in these 4-h experiments, the tissue could be considered semi-infinite. The constant  $B_1$  reflects the uptake of drug into tissue, and is a measure of the degree of binding to fixed proteins and partitioning into lipid. Note that this constant does not impact the rate of drug transfer through the tissue ( $D_{\text{art}}$ , eq. 3). The distribution in each artery was fit separately and the average and SD was calculated for each experimental condition (Table 1). ANOVA showed that regardless of which proteins carried paclitaxel to the blood vessel wall, the effective diffusivities in arterial tissue were indistinguishable at  $\sim 0.2 \mu\text{m}^2/\text{s}$ .

Compared with drugs that do not exhibit such binding, the effective diffusivity of paclitaxel is much lower than would be predicted from its molecular weight. For example, heparin is extremely hydrophilic and does not partition into elements of the arterial wall as does paclitaxel. The effective diffusivities of paclitaxel in arterial media are  $\sim 40$  times slower than that of heparin ( $7.7 \mu\text{m}^2/\text{s}$ ),<sup>23</sup> despite the smaller molecular weight of the former (854 Da) compared with that of the latter (14 kDa). The relative slow permeation of paclitaxel in tissues, despite its much smaller size, suggests that the repetitive binding and release of this drug to and from fixed arterial elements competes with migration down its concentration gradient, resulting in a lower effective diffusivity (Fig. 1, step III). Thus, the mechanisms of transarterial transport are extremely different for hydrophobic and hydrophilic compounds with such disparate lipophilicity, protein binding, and partitioning into fat.

The protein carriers in the lumen do impact the overall uptake of drug into the tissue. The tissue concentration normalized by the endovascular concentration is highest without proteins, lower in the presence of albumin, and lowest when administered in serum (Fig. 3). These proteins are likely to be excluded from the arterial wall in a size-dependent fashion from increased steric interactions on larger molecules. Drug that is bound to carriers will be excluded unless the protein enters the tissue, which they do in small amounts, or the drug dissociates. Thus, although proteins bring more drug to the vessel wall, they tend to keep it within the circulation.

### In Vivo versus Ex Vivo

Studies were performed in an *ex vivo* perfusion apparatus that allowed us to precisely control the applied concentration of drug and carrier, and to examine calf carotid arteries that are thick enough to permit transmural sectioning for determination of drug distribution profiles. To verify that the described mechanisms are valid *in vivo* we determined whole-artery deposition of paclitaxel after delivery of drug to the intact rat carotid artery in either protein free buffer or in serum. For comparison, the whole-artery deposition of paclitaxel was determined in calf carotid arteries in our *ex vivo* perfusion apparatus. Although the paclitaxel uptake was 3.5-fold greater *in vivo* than *ex vivo*, in both cases delivery in protein-free buffer resulted in an almost 9-fold more efficient uptake than when delivered in calf serum (Fig. 4). The consistent difference between the presence and absence of serum proteins suggests that the same mechanisms govern paclitaxel uptake and distribution *ex vivo* and *in vivo*. The serum proteins, when present, increase the amount of drug applied to the artery by increasing the effective solubility, yet limit the penetration and concentration of drug within the tissue through increased steric hindrance inside the arterial interstitium.

Physiologic pressure was maintained in these data, which added a convective component to the transmural transport of the soluble drug fraction in the interstitium of the arterial wall.<sup>23,26</sup> Because diffusive and convective forces are aligned, the transport may be augmented by physiologic pressure. However, movement by either mechanism occurs only on the small soluble interstitial fraction. Thus, the strong binding and partitioning of paclitaxel to the arterial wall overwhelms

this additional convective component to the transport.

## SUMMARY

Serum proteins influence the solubility and diffusivity of the hydrophobic drug paclitaxel. Through conjugation with these proteins, the amount of drug held in solution increases, but as a consequence, the transport is slowed in free solution and uptake into tissues is limited. We rigorously characterized the carrier-mediated phenomenon with paclitaxel both in free solution and within arterial tissues. These data demonstrate and quantify the mechanisms by which the local tissue pharmacokinetics differ for hydrophobic and hydrophilic drugs and may rationally guide their use in the treatment of proliferative vascular diseases.

## ACKNOWLEDGMENTS

This study was supported in part by grants from the National Institutes of Health (GM/HL 49039, 60407), the Stanley J. Sarnoff Endowment for Cardiovascular Science, the Whitaker Foundation Graduate Fellowship in Biomedical Engineering, and Allan and Luanne Reed's support of the Health Sciences and Technology Endowment at the Massachusetts Institute of Technology. We are grateful to Yoram Richter for his analytical and statistical assistance, and to Angiotech Pharmaceuticals, Inc. for providing radiolabeled paclitaxel. Elazer R. Edelman is an Established Investigator of the American Heart Association.

## REFERENCES

1. Ip JH, Fuster V, Badimon L, Badimon J, Taubman MB, Chesebro JH. 1990. Syndromes of accelerated atherosclerosis: Role of vascular injury and smooth muscle proliferation. *J Am Coll Cardiol* 15:1667–1687.
2. Ellis SG, Roubin GS, King SB, Douglas JS, Weintraub WS, Thomas RG, Cox WR. 1988. Angiographic and clinical predictors of acute closure after native vessel coronary angioplasty. *Circulation* 77:372–379.
3. Clowes AW, Karnovsky MJ. 1977. Suppression by heparin of smooth muscle cell proliferation in injured arteries. *Nature* 265:625–626.
4. Clowes AW, Clowes MM. 1985. Kinetics of cellular proliferation after arterial injury. II: Inhibition of smooth muscle cell growth by heparin. *Lab Invest* 52:611–616.
5. Guyton J, Rosenberg R, Clowes A, Karnovsky M. 1980. Inhibition of rat arterial smooth muscle cell proliferation by heparin I. In vivo studies with anticoagulant and non-anticoagulant heparin. *Circ Res* 46:625–634.
6. Villa A, Guzman L, Chen W, Golomb G, Levy R, Topol E. 1994. Local delivery of dexamethasone for prevention of neointimal proliferation in a rat model of balloon angioplasty. *J Clin Invest* 93:1243–1249.
7. Muller DWM, Golomb G, Gordon D, Levy RJ. 1994. Site-specific dexamethasone delivery for the prevention of neointimal thickening after vascular stent implantation. *Coron Art Dis* 5:435–442.
8. Powell JS, Clozel JP, Muller RKM, Kuhn H, Hefti F, Hosang M, Baumgartner HR. 1989. Inhibitors of angiotensin-converting enzyme prevent myointimal proliferation after injury. *Science* 245:186–188.
9. Lambert T, Dev V, Rechavia E, Forrester JS, Litvack F, Eigler NL. 1994. Localized arterial wall drug delivery from a polymer-coated removable metallic stent. Kinetics, distribution, and bioactivity of forskolin. *Circulation* 90:1003–1011.
10. Muller DWM, Ellis SG, Topol EJ. 1991. Colchicine and antineoplastic therapy for the prevention of restenosis after percutaneous coronary interventions. *J Am Coll Cardiol* 17:126B–131B.
11. Gradus-Pizlo I, Wilensky RL, March KL, Fineberg N, Michaels M, Sandusky GE, Hathaway DR. 1995. Local delivery of biodegradable microparticles containing colchicine or a colchicine analogue: Effects on restenosis and implications for catheter-based drug delivery. *J Am Coll Cardiol* 26:1549–1557.
12. Speir E, Epstein S. 1992. Inhibition of smooth muscle proliferation by an antisense oligodeoxynucleotide targeting the messenger RNA encoding proliferating cell nuclear antigen. *Circulation* 86:538–547.
13. Simons M, Edelman ER, Langer R, DeKeyser JL, Rosenberg RD. 1992. Antisense *c-myc* oligonucleotides inhibit intimal arterial smooth muscle accumulation *in vivo*. *Circulation* 85:69–73.
14. Axel DI, Kunert W, Goggelmann C, Oberhoff M, Herdeg C, Kuttner A, Wild DH, Brehm BR, Riessen R, G. Koveker KRK. 1997. Paclitaxel inhibits arterial smooth muscle cell proliferation and migration *in vitro* and *in vivo* using local drug delivery. *Circulation* 96:636–645.
15. Sollott SJ, Cheng L, Pauly RR, Jenkins GM, Monticone RE, Kuzuya M, Froehlich JP, Crow MT, Lakatta EG, Rowinsky EK, Kinsella JL. 1995.

- Taxol inhibits neointimal smooth muscle cell accumulation after angioplasty in the rat. *J Clin Invest* 95:1869–1876.
16. Strauss BH, Wilson RA, Houten Rv, Suylen Rv, Murphy ES, Escaned J, Verdouw PD, Serruys PW, Giessen WJvd. 1994. Late effects of locally delivered mitomycin c on formation of neointima and on vasomotor response to acetylcholine. *Coron Art Dis* 5:633–641.
  17. Hansson GK, Holm J. 1991. Interferon-gamma inhibits arterial stenosis after injury. *Circulation* 84:1266–1272.
  18. Fox JR, Wayland H. 1979. Interstitial diffusion of macromolecules in the rat mesentery. *Microvasc Res* 18:255–276.
  19. Swabb EA, Wei J, Gullino M. 1974. Diffusion and convection in normal and neoplastic tissues. *Cancer Research* 34:2814–2822.
  20. Jain RK. 1985. Transport of Macromolecules in tumor microcirculation. *Biotech Prog* 1:81–94.
  21. Nakamura Y, Wayland H. 1975. Macromolecular transport in the cat mesentery. *Microvasc Res* 9:1–21.
  22. Lovich MA, Edelman ER. 1996. Computational simulations of local vascular heparin deposition and distribution. *Am J Physiol* 271:H2014–H2024.
  23. Lovich MA, Edelman ER. 1995. Mechanisms of transmural heparin transport in the rat abdominal aorta after local vascular delivery. *Circ Res* 77:1143–1150.
  24. Lovich MA, Edelman ER. 1996. Tissue average binding and equilibrium distribution: an example with heparin in arterial tissues. *Biophys J* 70:1553–1559.
  25. Lovich MA, Brown L, Edelman ER. 1997. Drug clearance and arterial uptake following local perivascular delivery to the rat carotid artery. *J Am Coll Cardiol* 29:1645–1650.
  26. Lovich MA, Philbrook M, Sawyer S, Weselcouch E, Edelman ER. 1998. Arterial Heparin Deposition: Role of Diffusion, Convection, and Extravascular Space. *Am J Physiol* 275:H2236–H2242.
  27. Edelman ER, Lovich MA. 1998. Drug delivery models transported to a new level. *Nature Biotechnology* 16:136–137.
  28. Edelman ER, Karnovsky JM. 1994. Contrasting effects of the intermittent and continuous administration of heparin in experimental restenosis. *Circulation* 89:770–776.
  29. Pardridge WM, Sakiyama R, Fierer G. 1983. Transport of propranolol and lidocaine through the rat blood-brain barrier. Primary role of globulin-bound drug. *J Clin Invest* 71:900–908.
  30. Lemaire M, Pardridge WM, Chaudhuri G. 1988. Influence of blood components on the tissue uptake indices of cyclosporin in rats. *J Pharmacol Exp Ther* 244:740–743.
  31. Tillement JP, Urien S, Chaumet-Riffaud P, Riant P, Bree F, Morin D, Albengres E, Barre J. 1988. Blood binding and tissue uptake of drugs. Recent advances and perspectives. *Fundam Clin Pharmacol* 2:223–238.
  32. Herve F, Urien S, Albengres E, Duche JC, Tillement JP. 1994. Drug binding in plasma. A summary of recent trends in the study of drug and hormone binding. *Clin Pharmacokinet* 26:44–58.
  33. Belaiba R, Riant P, Urien S, Bree F, Albengres E, Barre J, Tillement JP. Blood binding and tissue transfer of drugs: The influence of  $\alpha_1$  acid glycoprotein binding. In: Baumann P, Eap CB, Muller WE, Tillement JP, editors. *Alpha-1-Acid glycoprotein: Genetics, biochemistry, physiological functions, and pharmacology*. New York: Alan R. Liss, Inc., 1989, pp 287–305.
  34. Straubinger RM. Biopharmaceutics of paclitaxel (Taxol): Formulation, activity, and pharmacokinetics. In: Suffness M, editor. *Taxol: Science and applications*, Boca Raton: CRC Press. 1995, pp. 237–257.
  35. Liggins RT, Hunter WL, Burt HM. 1997. Solid-state characterization of paclitaxel. *J Pharm Sci* 86:1458–1463.
  36. Sharma U, Balasubramanian SV, Straubinger RM. 1995. Pharmaceutical and physical properties of paclitaxel (Taxol) complexes with cyclodextrins. *J Pharm Sci* 84:1223–1230.
  37. Creel C, Lovich MA, Edelman ER. 2000. Arterial paclitaxel distribution and deposition. *Circ Res* 86:879–884.
  38. Bratzler RL, Chisolm GM, Colton CK, Smith KA, Zilvermit DB, Lees RS. 1977. The distribution of labeled albumin across the rabbit thoracic aorta in vivo. *Circ Res* 40:182–190.
  39. Phelps RA, Putnam FW. Chemical composition and molecular parameters of purified plasma proteins. In: Putnam FW, editor. *The plasma proteins*. New York: Academic Press. 1960, vol. 1, pp. 143–178.
  40. Kumar GN, Walle K, Bhalla KN, Walle T. 1993. Binding of taxol to human plasma, albumin and alpha1-acid glycoprotein. *Res Commun Chem Path Pharmacol* 80:337–344.
  41. Matthew AE, Mejillano MR, Nath JP, Himes RH, Stella VJ. 1992. Synthesis and evaluation of some water-soluble prodrugs and derivatives of Taxol with antitumor activity. *J Med Chem* 35:145.
  42. Tarr BD, Yalkowsky SH. 1987. A new parenteral vehicle for the administration of some poorly water soluble anti-cancer drugs. *J Parenteral Sci Technol* 41:31–33.
  43. Swindell CS, Krauss NE, Horwitz SB, Ringel I. 1991. Biologically active taxol analogues with a deleted A-ring side chain substituents and variable c-2' configurations. *J Med Chem* 34:1176–1184.

44. Granath KA, Kvist BE. 1967. Molecular weight distribution analysis by gel chromatography on sephadex. *J Chromatogr* 28:69–81.
45. Crank J. 1998. *The mathematics of diffusion*. Oxford: Clarendon Press.